

This copy is for your personal, non-commercial use only.

If you wish to distribute this article to others, you can order high-quality copies for your colleagues, clients, or customers by [clicking here](#).

Permission to republish or repurpose articles or portions of articles can be obtained by following the guidelines [here](#).

The following resources related to this article are available online at www.sciencemag.org (this information is current as of May 27, 2010):

Updated information and services, including high-resolution figures, can be found in the online version of this article at:

<http://www.sciencemag.org/cgi/content/full/328/5981/1031>

Supporting Online Material can be found at:

<http://www.sciencemag.org/cgi/content/full/science.1183057/DC1>

This article **cites 32 articles**, 17 of which can be accessed for free:

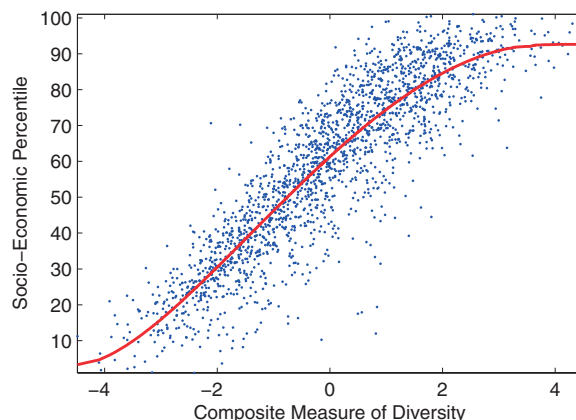
<http://www.sciencemag.org/cgi/content/full/328/5981/1031#otherarticles>

This article appears in the following **subject collections**:

Medicine, Diseases

<http://www.sciencemag.org/cgi/collection/medicine>

Fig. 2. The relation between social network diversity and socioeconomic rank. Diversity was constructed as a composite of Shannon entropy and Burt's measure of structural holes, by using principal component analysis. A fractional polynomial was fit to the data.



Although both social and spatial network diversity scores were strongly correlated with IMD rank ($r = 0.73$ and $r = 0.58$, respectively), we found a weaker positive correlation present using number of contacts ($r = 0.44$) and a negative correlation for communication volume ($r = -0.33$). For example, whereas inhabitants of Stoke-on-Trent, one of the least prosperous regions in the UK, averaged a higher monthly call volume than the national average, they have one of the lowest diversity scores in the country. Similarly prosperous Stratford-upon-Avon has inhabitants with extremely diverse networks, despite no more communication than the national average.

The strong association between diversity and IMD rank persists using other network diversity metrics, including Burt's measure of "structural holes" (9). A structural hole is a missing relation between any two of a node's neighbors, creating an open triad. Burt's seminal work showed that remuneration within an organization increases with the number of structural holes that surround a node. Our results show that this relation scales to the level of communities, whose socioeconomic opportunities increase with the number of structural holes in the ego networks of the members ($r = 0.72$). Moreover, a composite measure constructed via principal component analysis was an even better predictor of economic development than either component alone, as illustrated in Fig. 2 ($r = 0.78$).

By coupling the most complete population-level social network studied to date with community-level economic outcomes, we were able to validate a central assumption that is widely accepted in network science but was untested at the population level: Do more diverse ties provide greater access to social and economic opportunities? Although the causal direction of this relation—whether network diversity promotes opportunity or economic development leads to more diversified contacts—cannot be established, social network diversity seems to be at the very least a strong structural signature for the economic development of a community. On a population level, the surprisingly strong correspondence we discovered between the structure of social contacts and the economic well-being of populations highlights the potential benefit of socially targeted policies for economic development. However, additional research will be required to derive reliable

policy implications. In particular, establishing the causal mechanisms underlying the observed correspondence between network diversity and economic development may require additional longitudinal social network and economic data (26–28).

References and Notes

1. M. Newman, *SIAM Rev.* **45**, 167 (2003).
2. S. Page, *The Difference: How the Power of Diversity Creates Better Groups, Firms, Schools, and Societies* (Princeton Univ. Press, Princeton, NJ, 2007).
3. M. Granovetter, *Sociol. Theory* **1**, 201 (1983).
4. Y. Bian, *Am. Sociol. Rev.* **62**, 366 (1997).
5. M. Granovetter, *Am. J. Sociol.* **78**, 1360 (1973).
6. R. Fernandez, N. Weinberg, *Stanford GSB Research Paper Series no. 1382*, 1 (1994).
7. D. Brass, *Adm. Sci. Q.* **29**, 518 (1984).
8. D. Brass, *Acad. Manage. J.* **28**, 327 (1985).
9. R. Burt, *Structural Holes: The Social Structure of Competition* (Harvard Univ. Press, Cambridge, MA, 1992).
10. P. Marsden, J. Hurlbert, *Soc. Forces* **66**, 1038 (1988).
11. N. Lin, W. Ensel, J. Vaughn, *Am. Sociol. Rev.* **46**, 393 (1981).
12. H. Flap, N. Degraaf, *Netherlands J. Sociol.* **22**, 145 (1986).
13. N. Degraaf, H. Flap, *Soc. Forces* **67**, 453 (1988).
14. B. Wegener, *Am. Sociol. Rev.* **56**, 60 (1991).
15. J. Podolny, J. Baron, *Am. Sociol. Rev.* **62**, 673 (1997).
16. M.-D. Seidel, J. Polzer, K. Stewart, *Adm. Sci. Q.* **45**, 1 (2000).
17. S. Seibert, M. Kraimer, R. Liden, *Acad. Manage. J.* **44**, 219 (2001).
18. H. Aldrich, C. Zimmer, in *The Art and Science of Entrepreneurship*, D. L. Sexton, R. W. Smilor, Eds. (Ballinger Publishing, Cambridge, MA, 1986), pp. 3–24.
19. P. Dubini, H. Aldrich, *J. Bus. Venturing* **6**, 305 (1991).
20. M. Burkhardt, D. Brass, *Adm. Sci. Q.* **35**, 104 (1990).
21. D. Brass, M. Burkhardt, *Acad. Manage. J.* **36**, 441 (1993).
22. Previous studies have used longitudinal designs to test the hypothesized one-way causal direction between network position and individual economic benefits. These results suggest a similar causal direction at the population level, but our national data do not allow us to test for causal direction, and we cannot rule out the possibility that economic advantages may also lead to changes in network structure.
23. The anonymized call logs were recorded by the network operator as required by law and for billing purposes and not for the purpose of this project. Although these communication data and the exact location of the telephone exchanges are not publicly available, the regional aggregates are available from the first author.
24. Department of Communities and Local Government, *Indices of Deprivation 2004—Summary (revised)* (Department of Communities and Local Government, Stationery Office, London, 2004); www.communities.gov.uk/archived/general-content/communities/indicesofdeprivation/indicesofdeprivation/?view=Standard.
25. The 2004 IMD was constructed before the 2005 telephone call logs were recorded. We assume that the 2004 IMD rankings are relatively constant and, therefore, make no causal inference from the temporal order. Additionally, exchange areas can also be scored with specific IMD components, such as education. Higher education may promote more diverse network ties and lead to jobs with higher income, which might account for part of the correspondence between IMD and network diversity.
26. S. Aral, L. Muchnik, A. Sundararajan, *Proc. Natl. Acad. Sci. U.S.A.* **106**, 21544 (2009).
27. S. Curran, M. O. Jackson, P. Pin, *Proc. Natl. Acad. Sci. U.S.A.* **107**, 4857 (2010).
28. C. Manski, *Rev. Econ. Stud.* **60**, 531 (1993).
29. Office for National Statistics, *Super Output Area Boundaries* (Her Majesty's Stationery Office, London, 2004).
30. This work was supported by the Santa Fe Institute, the U.S. NSF (BCS-0537606), and British Telecom.

Supporting Online Material

www.sciencemag.org/cgi/content/full/328/5981/1029/DC1
Materials and Methods

Figs. S1 to S6

References

4 January 2010; accepted 14 April 2010

10.1126/science.1186605

Coadministration of a Tumor-Penetrating Peptide Enhances the Efficacy of Cancer Drugs

Kazuki N. Sugahara,^{1*} Tambat Teesalu,^{1*} Priya Prakash Karmali,² Venkata Ramana Kotamraju,¹ Lilach Agemy,¹ Daniel R. Greenwald,³ Erkki Ruoslahti^{1,2,†}

Poor penetration of anticancer drugs into tumors can be an important factor limiting their efficacy. We studied mouse tumor models to show that a previously characterized tumor-penetrating peptide, iRGD, increased vascular and tissue permeability in a tumor-specific and neuropilin-1-dependent manner, allowing coadministered drugs to penetrate into extravascular tumor tissue. Importantly, this effect did not require the drugs to be chemically conjugated to the peptide. Systemic injection with iRGD improved the therapeutic index of drugs of various compositions, including a small molecule (doxorubicin), nanoparticles (nab-paclitaxel and doxorubicin liposomes), and a monoclonal antibody (trastuzumab). Thus, coadministration of iRGD may be a valuable way to enhance the efficacy of anticancer drugs while reducing their side effects, a primary goal of cancer therapy research.

The therapeutic efficacy of many anticancer drugs is limited by their poor penetration into tumor tissue and by their adverse ef-

fects on healthy cells, which limits the dose of drug that can be safely administered to cancer patients. In solid tumors, many anticancer drugs

penetrate only 3 to 5 cell diameters from the blood vessels, leading to reduced efficacy and the development of drug resistance (1, 2). We recently identified a tumor-penetrating peptide, iRGD (CRGDK/RGPD/EC) (3), that, when chemically conjugated to a drug, can carry the drug deep into extravascular tumor tissue (4). Like conventional RGD peptides, iRGD homes to tumors by initially binding to α_v integrins that are specifically expressed on the endothelium of tumor vessels (4–6). iRGD is then proteolytically cleaved in the tumor to produce CRGDK/R. The truncated peptide loses much of its integrin-binding activity, but gains affinity for neuropilin-1 (NRP-1) because of the C-terminal exposure of a conditional C-end Rule (CendR) motif (R/KXXR/K) (7). The NRP-1 binding triggers tissue penetration, which

is tumor-specific because the cleavage requires earlier binding of the peptide to integrins. These features confer on iRGD a tumor-specific tissue penetration activity. Here we explore whether the iRGD peptide can enhance cancer drug delivery and activity when it is administered as a combination therapy with drugs that are not chemically conjugated to it. This would be advantageous because already approved drugs could be used without creating a new chemical entity, and because coupling often interferes with drug activity.

The activity of peptides and proteins that bind to NRP-1 through a C-terminal CendR motif can be demonstrated by monitoring vascular permeability (7–9). We examined whether the CendR-triggered vascular permeability may play a role in the iRGD tumor-penetrating activities using human tumor xenografts growing in immunodeficient mice and in de novo mouse tumors growing in transgenic mice. Indeed, chemically synthesized iRGD peptide, when co-injected with the albumin-binding dye Evans blue (10–12), caused tumor-specific accumulation of the dye in all five tumor models that we tested (one breast cancer, two prostate cancers, and two pancreatic adenocarcinomas), including secondary invasion sites and disseminated tumors (figs. S1A and S2, A and B). The accumulation of the dye was dependent on the dose of iRGD administered and peaked at ~400%

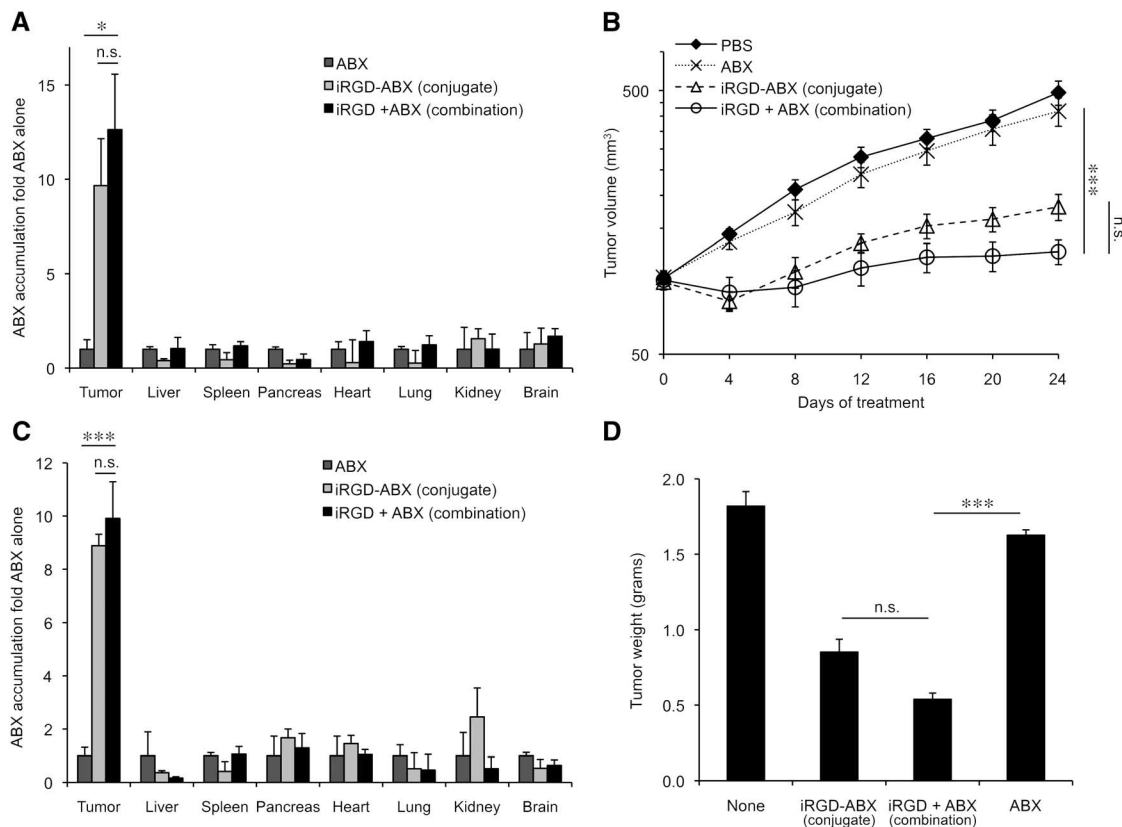
more than the dye alone (fig. S1B). Non-CendR RGD peptides, RGD-4C (CDCRGDCFC) (13) and cyclo(-RGDfK-) (14), and a scrambled iRGD with no CendR motif (CRGDDGPKC) (here, bold letters indicate the position swap of amino acids) did not increase the permeability (figs. S1C and S2C). Preinjection of an antibody to NRP-1 (anti-NRP-1) inhibited the iRGD-induced permeability (fig. S1D). CRGDK, the truncated iRGD peptide with an exposed CendR motif, enhanced local vascular permeability in the skin in a dose-dependent manner (fig. S3) (7). When injected systemically, CRGDK increased permeability in the tumors, as well as in the lungs and heart. CRGDK was somewhat selective for the tumors, probably because of its residual affinity to integrins and the generally high expression of NRP-1 in tumors (fig. S1C) (4, 7, 15).

The tumor-specific increase in tissue access mediated by iRGD suggests a way of improving the delivery of compounds to tumor parenchyma (fig. S4). A fluorescein-labeled non-CendR peptide CRGDC (FAM-CRGDC; 1.3 kD), which minimally penetrates tumors by itself (4, 16), showed enhanced extravascular distribution upon iRGD co-injection (fig. S5A). The co-injection caused a 300% increase in both of the FAM-CRGDC-positive areas (fig. S5B) and the spreading of FAM-CRGDC (fig. S5C) in the tumors. We ob-

¹Vascular Mapping Laboratory, Center for Nanomedicine, Sanford-Burnham Medical Research Institute at University of California at Santa Barbara, Biology II Building, University of California, Santa Barbara, CA 93106–9610, USA. ²Cancer Research Center, Sanford-Burnham Medical Research Institute, 10901 North Torrey Pines Road, La Jolla, CA 92037, USA. ³Santa Barbara Hematology Oncology Medical Group, Cancer Center of Santa Barbara, 540 West Pueblo Street, Santa Barbara, CA 93105, USA.

*These authors contributed equally to this work.
†To whom correspondence should be addressed. E-mail: ruoslahti@burnham.org

Fig. 1. Comparison of the drug-delivery efficiency of the iRGD combination regimen and conjugated drug delivery. **(A and C)** Nab-paclitaxel (ABX) quantification in orthotopic human breast tumor (BT474) (A) and human prostate tumor (22Rv1) (C) xenograft models. ABX with free iRGD (combination), ABX coated with iRGD (conjugate), or ABX alone, was intravenously injected into tumor-bearing mice. Three hours later, ABX was captured from tumor extracts with an antitaxol antibody, followed by detection with a human albumin antibody. $n = 3$ mice per group for both (A) and (C). **(B and D)** Long-term treatment of tumor mice with ABX. Mice bearing orthotopic BT474 (B) or 22Rv1 (D) tumors were intravenously injected with the indicated ABX formulations every other day at 3 mg paclitaxel/kg per injection or with phosphate-buffered saline (PBS) only. The treatment was continued for both 24 (B) and 16 days (D). $n = 8$ per group (B) and 9 per group (D), respectively. Statistical analyses were



performed with Student's *t* test in (A) and (C) and analysis of variance (ANOVA) in (B) and (D). Error bars denote mean \pm SEM. n.s., not significant; * $P < 0.05$; *** $P < 0.001$.

tained similar results with 3- and 10-kD dextrans (fig. S5). Two nanoparticles, iron oxide nanoworms (17) and T7 phage, also extravasated and showed enhanced accumulation in the tumor upon iRGD co-injection (fig. S6). These results show that iRGD can increase the tumor accumulation of compounds with different sizes and chemical properties.

Intravenously injected molecules and nanoparticles slowly extravasate into perivascular areas in tumor tissue through passive leakage (18, 19). The rapid and deep tumor penetration of the probes co-injected with iRGD prompted us to study the possibility that CendR might be triggering an active transport process. To exclude circulatory effects, we used fresh explants of PPC-1 human prostate tumors in this study. Phage particles expressing the iRGD peptide on their surface (4), but not inert control phage, penetrated into PPC-1 prostate cancer xenograft explants, advancing ~4 mm in 90 min (fig. S7). The penetration was inhibited by anti-NRP-1, sodium azide, and by lowering the temperature, suggesting that the penetration process was NRP-1- and energy-dependent. Importantly, inert phage penetrated into the explants in the presence of iRGD, but not with a control peptide.

To study the effect of iRGD on drug delivery and efficacy, we administered the peptide as a combination therapy with several types of cancer drugs to mice bearing human tumor xenografts. We first compared the delivery efficiency of this combination regimen to that of the cancer drug

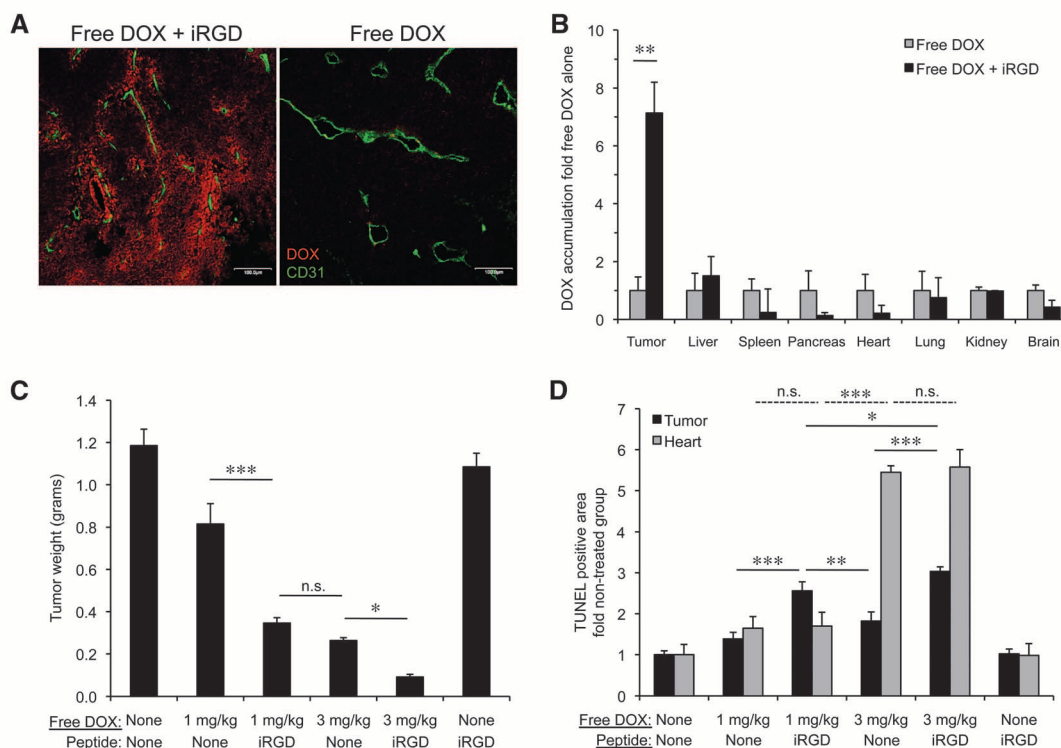
alone and to that of the cancer drug when it was chemically conjugated to the peptide. When intravenously injected with iRGD, Nab-paclitaxel [abraxane (ABX)], a 130-nm nanoparticle consisting of albumin-embedded paclitaxel (4, 20), accumulated 12-fold more in orthotopic BT474 human breast tumors than ABX given alone and penetrated far from the tumor vessels (Fig. 1A and fig. S8). Treatment of mice every other day with the ABX/iRGD combination inhibited the growth of BT474 tumors, which were resistant to equivalent doses of ABX alone (Fig. 1B). The combination was slightly more effective than the conjugated drug in inhibiting tumor growth, as well as in tumor accumulation, but the differences did not reach statistical significance. Similar results were obtained in orthotopic 22Rv1 human prostate tumors (Fig. 1, C and D).

We next used another clinically relevant system to evaluate the effect of the combination therapy on the therapeutic index (a comparison of the dose needed to elicit a therapeutic effect to the lethal dose). Doxorubicin (DOX) and DOX liposomes have clinical activity in a number of tumor types, including prostate cancer (21). We treated orthotopic 22Rv1 tumors with a combination of iRGD and DOX (0.6 kD). Free DOX co-injected with iRGD penetrated the tumors and accumulated sevenfold more in the tumors than DOX given alone (Fig. 2, A and B). The combination therapy that included 1 mg/kg DOX was as potent as 3 mg/kg DOX alone, a dose that reaches the cumulative maximum tolerated dose (Fig. 3C)

(22). Combining iRGD with 3 mg/kg of DOX potentiated the activity of DOX, inducing nearly complete tumor-growth inhibition (Fig. 2C). Tumors from both the 1- and 3-mg/kg DOX groups combined with iRGD showed stronger terminal deoxynucleotidyl transferase-mediated deoxyuridine triphosphate nick end labeling (TUNEL) staining, an indicator of cell death, than tumors treated with 3-mg/kg DOX alone (Fig. 2D). Cardiotoxicity, the main dose-limiting toxicity of DOX, is manifested as cardiomyocyte apoptosis (23). The iRGD combination had the same cardiotoxicity as an equivalent dose of DOX alone (Fig. 2D). The body-weight shift was also the same, whether DOX was given alone or combined with iRGD (fig. S9). Similar results were obtained with orthotopic 4T1 mouse breast tumors (figs. S9 and S10). iRGD alone at the dose used in the combination group showed no effect on tumor growth (Fig. 2C), supporting the notion that the effects of the combination are due to improved drug penetration.

We also tested DOX in a liposomal formulation (particle diameter = 120 nm). The results were similar to those with free DOX with regard to treatment efficacy (Fig. 3A), tumor accumulation of the drug (14-fold) (Fig. 3B), tumor penetration (fig. S11), and toxicity (Fig. 3C and fig. S9). In addition, we tested a non-CendR RGD in this system and found that it did not enhance the efficacy of the drug (Fig. 3A). These results indicate that, in comparison to drug administered alone, the iRGD combination therapy provides

Fig. 2. Enhanced antitumor effect of free DOX co-injected with iRGD. **(A and B)** Mice bearing orthotopic 22Rv1 human prostate tumors were intravenously injected with a mixture of DOX (10 mg/kg) and 4 μmol/kg of iRGD or PBS. Tumors and tissues were collected 1 hour later. *n* = 3 per group. In **(A)**, the tumors were sectioned and stained for blood vessels with anti-CD31, and the native fluorescence was used to detect DOX. Scale bars, 100 μm. In **(B)**, DOX in the tissues was quantified. **(C)** Mice bearing orthotopic 22Rv1 tumors implanted 2 weeks earlier received intravenous injections of DOX (1 or 3 mg/kg) or PBS, combined with 4 μmol/kg of iRGD or PBS, every other day. The tumors were harvested and weighed after 24 days of treatment. *n* = 10 per group. **(D)** TUNEL staining was performed on tumors and hearts from the treatment study and was quantified for positive staining. Statistical analyses were performed with Student's *t* test (**B**) and ANOVA (**C** and **D**). Error bars denote mean ± SEM. n.s., not significant; **P* < 0.05; ***P* < 0.01; ****P* < 0.001.



equivalent or better antitumor efficacy at a three-fold lower dose of the drug, with a commensurate reduction in toxicity. The results also show that this therapy regimen can be effective with drugs ranging in size from a small-molecular weight chemical (DOX) to nanoparticles (ABX, DOX liposomes).

Finally, we tested the iRGD-combination regimen in mice bearing tumors derived from BT474 human breast tumor cells, which over-express HER2/neu/ErbB2. This growth-factor receptor is the target of trastuzumab, a therapeutic monoclonal antibody in clinical use for the treatment of breast cancer (24, 25). Co-injection of iRGD resulted in a 14-fold increase in trastuzumab-positive areas within the tumor (Fig. 4A). An enzyme-linked immunosorbent assay (ELISA) showed that iRGD enhanced the accumulation of trastuzumab in the tumors 40-fold; this increase is probably due to enhanced access and binding of the antibody to the tumor cells (Fig. 4B). Combining trastuzumab with iRGD increased the drug potency at different trastuzumab dose levels (Fig. 4C). At a clinical dose (9 mg/kg), the combination eradicated all tumors in the mice, whereas the equivalent dose of trastuzumab alone only slowed tumor growth (Fig. 4C). The eradicated tumors did not relapse during a 2-week observation period after the treatment was stopped.

The iRGD-mediated enhancement in drug penetration persisted even after more than 3 weeks of antibody treatment (figs. S12 and S13 for DOX and trastuzumab, respectively). However, the difference between the combination and the drug alone was smaller than with single dosing (compare fig. S13B with Fig. 4A). This explains the lack of a linear relation between the single dosing of the drugs, which gave 7- to 40-fold more drug accumulation, and the long-term treatments, which gave 3-fold stronger antitumor effects.

We also tested the possibility that iRGD might have the adverse effect of enhancing metastasis by promoting intravasation of tumor cells. No macroscopic metastases were found in mice treated with iRGD. Immunofluorescence for human leukocyte antigens and quantitative polymerase chain reaction measuring human genomic DNA revealed no human cells in organs collected at the end of the treatments, and the low levels of DNA were similar in the iRGD and control groups in the BT474 and 22Rv1 models (figs. S14 to S16) (26, 27).

The CendR penetration effect of the tumor-targeting methodology described here is distinct from the enhanced permeability and retention (EPR) effect: (i) EPR is a passive leakage from tumor vessels (18, 19), whereas the CendR penetration is receptor-mediated and energy-dependent. (ii) CendR is more effective than the EPR (fig. S5). (iii) CendR causes extravasation within minutes, whereas EPR requires 6 to 8 hours to peak (4, 18). (iv) Finally, CendR is effective with small molecules, whereas EPR is not (18). However, there may be a CendR component in EPR, be-

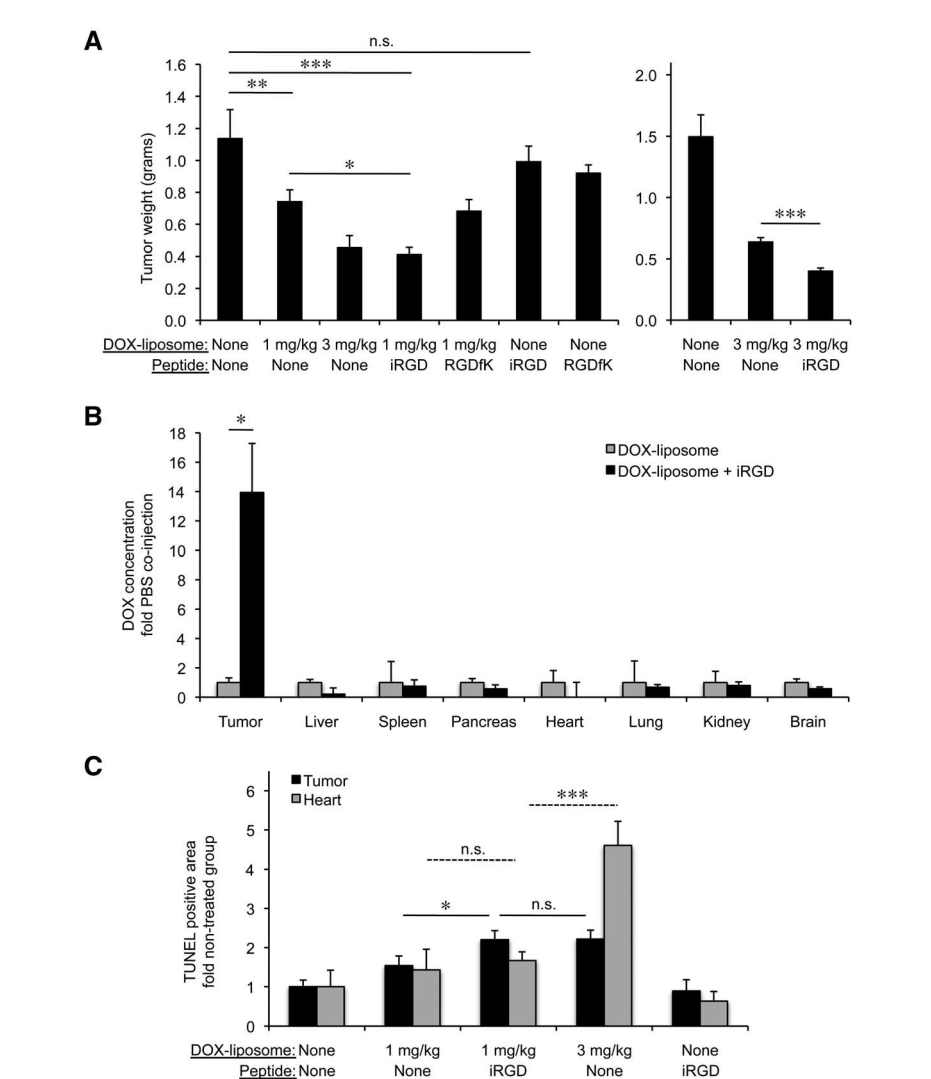


Fig. 3. Enhanced antitumor effect of DOX liposomes co-injected with iRGD. (A) Nude mice bearing orthotopic 22Rv1 human prostate tumors implanted 2 weeks earlier received daily intravenous injections of DOX liposomes (1 or 3 mg/kg) or PBS, combined with 2 μ mol/kg of iRGD or cyclo(-RGDfK-) or PBS. The tumors were harvested and weighed after 17 days of treatment. $n = 5$ per group (left panel); $n = 8$ per group (right panel). (B) Mice bearing orthotopic 22Rv1 tumors were intravenously injected with DOX liposomes (5 mg/kg), followed by 4 μ mol/kg of iRGD or PBS. The tumors and tissues were collected 3 hours later, and DOX in the tissues was quantified. $n = 3$ per group. (C) TUNEL staining was performed on tumors and hearts from the treatment study in (A) and was quantified for positive staining. Statistical analyses were performed with ANOVA [(A) left panel, and (C)] and Student's t test [(A) right panel, and (B)]. Error bars denote mean \pm SEM. n.s., not significant; * $P < 0.05$; ** $P < 0.01$; *** $P < 0.001$.

cause vascular endothelial growth factor-165 (VEGF-165), which is involved in the process, has an active CendR motif (7, 8, 18).

Administration of the tumor-penetrating peptide as a combination therapy bypasses two limitations of strategies in which the peptide is conjugated to the drug and delivered as a single agent: (i) The combination therapy does not require drug modification, which may impair drug activity, and (ii) the capacity of the system is not exceeded as easily as that of the conjugate delivery. Whereas delivery of the conjugated drug

depends on a finite number of target receptors, delivery of the peptide and drug as separate entities triggers a bulk transfer of the bystander drugs into the tumor tissue (28).

Attempts have been made to permeabilize tumor vasculature with VEGF and bradykinin for enhanced access of blood-borne molecules to tumor interstitium (29, 30), but the tumor specificity has been limited. One possible advantage of iRGD is that systemic administration of this peptide results in a tissue penetration effect that appears to be selective for tumors.

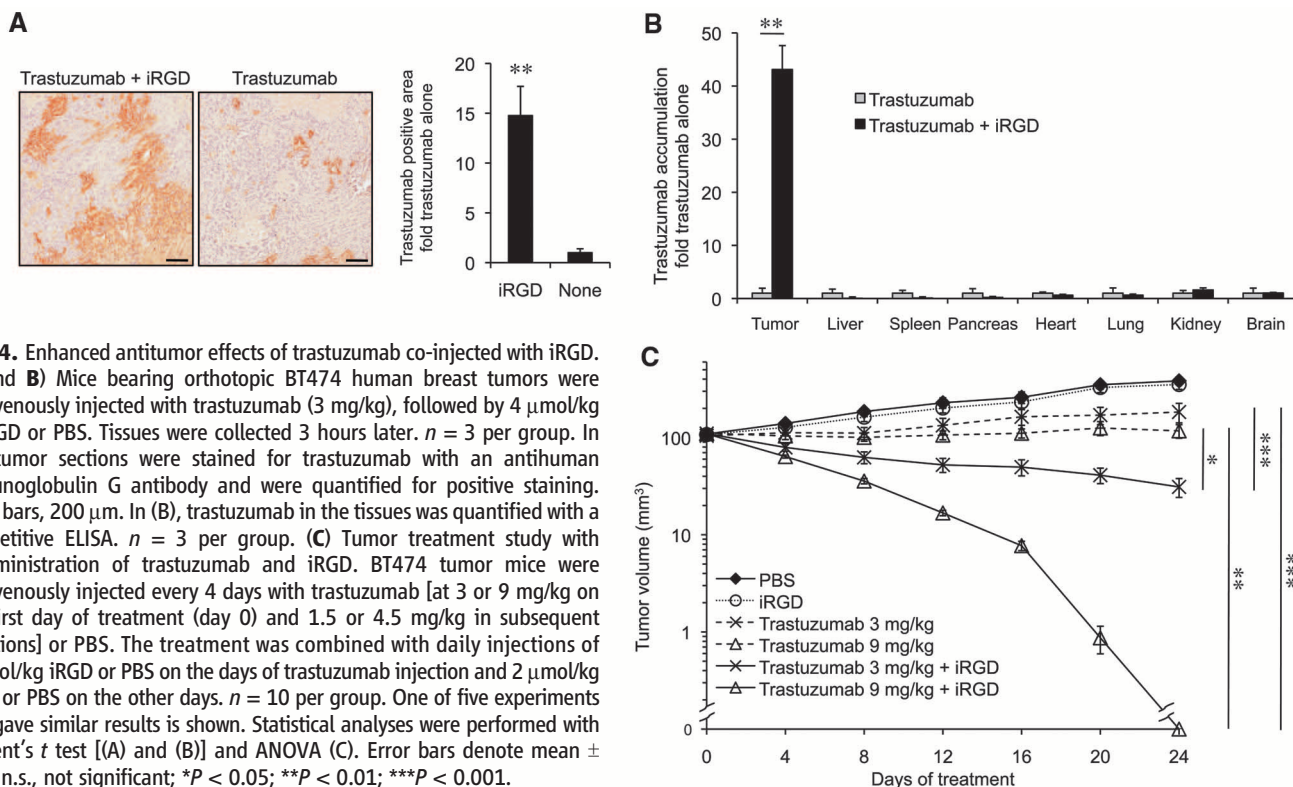


Fig. 4. Enhanced antitumor effects of trastuzumab co-injected with iRGD. (A and B) Mice bearing orthotopic BT474 human breast tumors were intravenously injected with trastuzumab (3 mg/kg), followed by 4 μ mol/kg of iRGD or PBS. Tissues were collected 3 hours later. $n = 3$ per group. In (A), tumor sections were stained for trastuzumab with an antihuman immunoglobulin G antibody and were quantified for positive staining. Scale bars, 200 μ m. In (B), trastuzumab in the tissues was quantified with a competitive ELISA. $n = 3$ per group. (C) Tumor treatment study with coadministration of trastuzumab and iRGD. BT474 tumor mice were intravenously injected every 4 days with trastuzumab [at 3 or 9 mg/kg on the first day of treatment (day 0) and 1.5 or 4.5 mg/kg in subsequent injections] or PBS. The treatment was combined with daily injections of 4 μ mol/kg iRGD or PBS on the days of trastuzumab injection and 2 μ mol/kg iRGD or PBS on the other days. $n = 10$ per group. One of five experiments that gave similar results is shown. Statistical analyses were performed with Student's t test [(A) and (B)] and ANOVA (C). Error bars denote mean \pm SEM. n.s., not significant; * $P < 0.05$; ** $P < 0.01$; *** $P < 0.001$.

We observed enhanced tumor-specific delivery of the 10 different compounds that we tested (from a 0.6-kD molecule up to a 130-nm particle), suggesting that the iRGD peptide might help improve the performance of a wide range of cancer drugs or tumor-imaging agents. Conceivably, the system can be further improved—for example, by employing multimeric iRGD, structurally stabilized iRGD, other tumor-homing CendR peptides (31–34) or peptide combinations, or by optimization of the dosing and administration schedules. Moreover, the efficacy and the specificity of the iRGD-mediated delivery remain to be shown in human patients. Human tumor vessels and tumor cells express the relevant α v integrins (5, 6) and NRP-1 (15), and iRGD and its fragment bind to them (4), suggesting that the system will translate to the treatment of human cancer. Increasing the therapeutic index of standard therapy may enhance efficacy while reducing toxicity, the primary goal of modern cancer therapy.

References and Notes

1. T. W. Hambley, W. N. Hait, *Cancer Res.* **69**, 1259 (2009).
2. A. I. Minchinton, I. F. Tannock, *Nat. Rev. Cancer* **6**, 583 (2006).
3. Single-letter abbreviations for the amino acid residues are as follows: A, Ala; C, Cys; D, Asp; E, Glu; F, Phe; G, Gly; H, His; I, Ile; K, Lys; L, Leu; M, Met; N, Asn; P, Pro; Q, Gln; R, Arg; S, Ser; T, Thr; V, Val; W, Trp; Y, Tyr; and X, any amino acid.
4. K. N. Sugahara *et al.*, *Cancer Cell* **16**, 510 (2009).

5. E. Ruoslahti, *Nat. Rev. Cancer* **2**, 83 (2002).
6. J. S. Desgrosellier, D. A. Cheresh, *Nat. Rev. Cancer* **10**, 9 (2010).
7. T. Teesalu, K. N. Sugahara, V. R. Kotamraju, E. Ruoslahti, *Proc. Natl. Acad. Sci. U.S.A.* **106**, 16157 (2009).
8. H. Jia *et al.*, *J. Biol. Chem.* **281**, 13493 (2006).
9. L. M. Acevedo, S. Barillas, S. M. Weis, J. R. Göthert, D. A. Cheresh, *Blood* **111**, 2674 (2008).
10. See supporting material on Science Online for methods and additional data. Statistical analyses are summarized in table S1.
11. A. A. Miles, E. M. Miles, *J. Physiol.* **118**, 228 (1952).
12. T. Murohara *et al.*, *Circulation* **97**, 99 (1998).
13. E. Koivunen, B. Wang, E. Ruoslahti, *Biotechnology (N.Y.)* **13**, 265 (1995).
14. E. A. Murphy *et al.*, *Proc. Natl. Acad. Sci. U.S.A.* **105**, 9343 (2008).
15. C. Pellet-Many, P. Frankel, H. Jia, I. Zachary, *Biochem. J.* **411**, 211 (2008).
16. E. Koivunen, D. A. Gay, E. Ruoslahti, *J. Biol. Chem.* **268**, 20205 (1993).
17. J. H. Park *et al.*, *Small* **5**, 694 (2009).
18. H. Maeda, J. Fang, T. Inutsuka, Y. Kitamoto, *Int. Immunopharmacol.* **3**, 319 (2003).
19. F. Yuan *et al.*, *Cancer Res.* **55**, 3752 (1995).
20. P. P. Karmali *et al.*, *Nanomedicine* **5**, 73 (2009).
21. R. Petrioli, A. I. Fiaschi, E. Francini, A. Pascucci, G. Francini, *Cancer Treat. Rev.* **34**, 710 (2008).
22. F. Pastorino *et al.*, *Clin. Cancer Res.* **14**, 7320 (2008).
23. O. J. Arola *et al.*, *Cancer Res.* **60**, 1789 (2000).
24. B. M. Fendly *et al.*, *Cancer Res.* **50**, 1550 (1990).
25. P. Carter *et al.*, *Proc. Natl. Acad. Sci. U.S.A.* **89**, 4285 (1992).
26. T. Primeau *et al.*, *Immunol. Res.* **32**, 109 (2005).
27. D. A. Tagle, F. S. Collins, *Hum. Mol. Genet.* **1**, 121 (1992).

28. E. Ruoslahti, S. N. Bhatia, M. J. Sailor, *J. Cell Biol.* **188**, 759 (2010).
29. W. L. Monsky *et al.*, *Cancer Res.* **59**, 4129 (1999).
30. K. L. Black, N. S. Ningaraj, *Cancer Control* **11**, 165 (2004).
31. J. A. Hoffman *et al.*, *Cancer Cell* **4**, 383 (2003).
32. J. A. Joyce *et al.*, *Cancer Cell* **4**, 393 (2003).
33. P. Laakkonen, K. Porkka, J. A. Hoffman, E. Ruoslahti, *Nat. Med.* **8**, 751 (2002).
34. K. Porkka, P. Laakkonen, J. A. Hoffman, M. Bernasconi, E. Ruoslahti, *Proc. Natl. Acad. Sci. U.S.A.* **99**, 7444 (2002).
35. We thank D. Hanahan for transgenic mice, R. M. Hoffman for the GFP-PC-3 cell line, M. J. Sailor and J.-H. Park for advice on the synthesis of iron oxide nanoworms, and E. Engvall for comments on the manuscript. This work was supported by grants CA104898, CA119414, CA119335, CA124427, CA115410, and CA30199 from the National Cancer Institute of the NIH and grants BC076050 and BC08544 from the U.S. Department of Defense. The authors and their institutions have patents on methods and compositions related to peptides and proteins with C-terminal elements and related to internalizing RGD peptides.

Supporting Online Material

www.sciencemag.org/cgi/content/full/science.1183057/DC1
 Materials and Methods
 SOM Text
 Figs. S1 to S16
 Table S1
 References

8 October 2009; accepted 25 March 2010
 Published online 8 April 2010;
 10.1126/science.1183057
 Include this information when citing this paper.